Likelihood-Free Gaussian Process for Regression

Yuta Shikuri

Yokohama, Japan shikuriyuta@gmail.com

Abstract

Gaussian process regression can flexibly represent the posterior distribution of an interest parameter given sufficient information on the likelihood. However, in some cases, we have little knowledge regarding the probability model. For example, when investing in a financial instrument, the probability model of cash flow is generally unknown. In this paper, we propose a novel framework called the likelihood-free Gaussian process (LFGP), which allows representation of the posterior distributions of interest parameters for scalable problems without directly setting their likelihood functions. The LFGP establishes clusters in which the value of the interest parameter can be considered approximately identical, and it approximates the likelihood of the interest parameter in each cluster to a Gaussian using the asymptotic normality of the maximum likelihood estimator. We expect that the proposed framework will contribute significantly to likelihoodfree modeling, particularly by reducing the assumptions for the probability model and the computational costs for scalable problems.

1 Introduction

Gaussian process regression (GPR) is a type of Bayesian nonparametric regression method that allows flexible representation of the posterior distribution of an interest parameter. However, some drawbacks to GPR have been published in the literature, and several reported studies have endeavored to overcome these limitations and extend the applicability of the method. The most severe drawback of GPR is the computational cost, which is $\mathcal{O}(n^3)$ for data size n. Moreover, the application of GPR to scalable problems has been a significant area of focus in current research. Variational inducing point (Titsias 2009; Candela and Rasmussen 2005) to minimize the Kullback-Leibler divergence for approximation of the posterior distribution is the most popular approach among methods for reducing the computational cost and is highlighted in some key works (Csat and Opper 2000; Shen and Seeger 2005; Bui and Turner 2014). Hensman et al. 2015 extended the likelihood to a non-Gaussian (i.e., free-form likelihood) by estimating the hyperparameters via an inducing point framework and Markov-Chain Monte Carlo procedures.

Preprint. Under review.

These works have contributed toward establishing a model for the posterior distribution of an interest parameter more flexibly. However, although free-form likelihood is a powerful tool, difficulties are encountered when the probability model is unknown. A typical example of this is the modeling of cash flows for investing in financial instruments (Thu and Xuan 2018; Sidehabi and Tandungan 2016). The demand for machine learning frameworks for algorithmic trading has been rapidly increasing in recent years. Traders are typically challenged to predict asset fluctuations using nonparametric models trained on large amounts of historical data. However, setting a probability model in such a situation is generally infeasible because the cash flows of financial instruments are quite complex.

Demands for likelihood-free modeling exist not only in the field of investments in financial instruments but also in other fields such as ecology and biology. To satisfy this demand, various types of likelihood-free inference methods have been proposed. One common idea among these methods is the representation of the probability distribution of targets via a repetitive process of simulating data and evaluating the discrepancies between the simulated and observed data (Gutmann and Corander 2016). In general, these methods have high computational cost, and we do not know how the parameters affect the discrepancy. Wood 2010 proposed a method that uses the synthetic likelihood to approximate the probability distribution of targets to a multivariate normal distribution using the central limit theorem. The computational cost in their method is more efficient than that of other methods. In addition, the discrepancies between the simulated and the observed data can be evaluated by comparing the individual maximum likelihood estimators for the data. Their method is simple and powerful, and our work is profoundly inspired by it. However, the utility of the method is limited to cases where the generative processes of the targets are clear, even though the likelihoods are intractable.

In this study, we propose a novel framework called the likelihood-free Gaussian process (LFGP), which represents the posterior distribution of an interest parameter in the form of a typical GPR without setting the likelihood function directly. We approximate the likelihood to a Gaussian using the asymptotic normalities of the maximum likelihood estimators. The concept of our approach is similar to that of (Wood 2010) from the perspective of the Gaussian

approximation. However, we do not assume any generative processes and focus on establishing clusters to obtain the maximum likelihood estimators of an interest parameter. In addition, we present a method to reduce the computational cost of setting up clusters. For the performance verification of the LFGP, we modeled some pseudo datasets and binary option (BO), which is a type of derivative instrument. Both methods and their results suggest that the LFGP is capable of representing the posterior distribution of an interest parameter even if only little knowledge on its probability model is available.

Contribution. We consider that the LFGP will contribute significantly to likelihood-free modeling, especially from the perspective of fewer assumptions for the probability models and lower computational costs for scalable problems.

2 Gaussian Process Regression

Gaussian processes (GPs) are distributions over functions (Rasmussen and Williams 2006), such that

$$f \sim \mathcal{GP}(\nu(\cdot), k(\cdot, \cdot)),$$
 (1)

where $\nu: \mathbb{R}^d \to \mathbb{R}$ is the mean function and $k: \mathbb{R}^d \times \mathbb{R}^d \to \mathbb{R}$ is the covariance function. Given an observed dataset $D = \{X, y\} = \{x_i, y_i\}_{i=1}^n$ with $x_i \in \mathbb{R}^d$, $y_i \in \mathbb{R}$, the posterior distribution of $f = \{f(x_i)\}_{i=1}^n$, $f: \mathbb{R}^d \to \mathbb{R}$ is stated as

$$p(f \mid D, \Lambda, \theta) \sim p(y \mid f, \Lambda) \mathcal{N}(f \mid \nu, K),$$
 (2)

where $\boldsymbol{\nu} = \{\nu(\boldsymbol{x_i})\}_{i=1}^n$, $[\boldsymbol{K}]_{s,t} = k(\boldsymbol{x_s}, \boldsymbol{x_t} \mid \boldsymbol{\theta})$, $\boldsymbol{\theta}$ are the hyperparameters of the prior distributions, $\boldsymbol{\Lambda} = \{\lambda(\boldsymbol{x_i})\}_{i=1}^n$ are the parameters of the probability model except for $\boldsymbol{f}, \lambda : \mathbb{R}^d \to \mathbb{R}^{u-1}$, and $u \in \mathbb{N}$ is the number of parameters of the probability model.

Training and Prediction. We maximize the log marginal likelihood,

$$\Lambda^*, \theta^* = \underset{\Lambda, \theta}{\operatorname{arg max}} \mathcal{L}(\Lambda, \theta \mid D), \tag{3}$$

$$\mathcal{L}(\boldsymbol{\Lambda}, \boldsymbol{\theta} \mid \boldsymbol{D}) = \log p(\boldsymbol{y} \mid \boldsymbol{X}, \boldsymbol{\Lambda}, \boldsymbol{\theta}). \tag{4}$$

If the probability model $p(\boldsymbol{y} \mid \boldsymbol{f}, \boldsymbol{\Lambda})$ is Gaussian, then we can analytically obtain the gradient of the log marginal likelihood $\mathcal{L}_{\text{Gauss}}(\sigma, \boldsymbol{\theta} \mid \boldsymbol{D})$ for the optimization. The form of $\mathcal{L}_{\text{Gauss}}(\sigma, \boldsymbol{\theta} \mid \boldsymbol{D})$ is given as

$$\mathcal{L}_{\text{Gauss}}(\sigma, \boldsymbol{\theta} \mid \boldsymbol{D}) = -\frac{1}{2} (\tilde{\boldsymbol{y}}^T \tilde{\boldsymbol{K}}^{-1} \tilde{\boldsymbol{y}} + \log |\tilde{\boldsymbol{K}}| + c), \quad (5)$$

where $c=n\log(2\pi), \tilde{\boldsymbol{y}}=\boldsymbol{y}-\boldsymbol{\nu}, \tilde{\boldsymbol{K}}=\boldsymbol{K}+\sigma^2\boldsymbol{I_n}, 0<\sigma\in\mathbb{R}$. In addition, the posterior distribution of $f^*=f(\boldsymbol{x^*})$ for a new input $\boldsymbol{x^*}\in\mathbb{R}^d$ is Gaussian. Its mean and variance are given as

$$\mathbb{E}[f^* \mid \boldsymbol{D}, \sigma^*, \boldsymbol{\theta}^*] = \nu(\boldsymbol{x}^*) + \boldsymbol{k}_*^T \tilde{\boldsymbol{K}}_*^{-1} \tilde{\boldsymbol{y}}, \tag{6}$$

$$\operatorname{Var}[f^* \mid \boldsymbol{D}, \sigma^*, \boldsymbol{\theta}^*] = k_{**} - \boldsymbol{k}_{*}^T \tilde{\boldsymbol{K}}_{*}^{-1} \boldsymbol{k}_{*}, \tag{7}$$

where $\tilde{K}_* = K_* + \sigma^{*2} I_n$, $[K_*]_{s,t} = k(x_s, x_t | \theta^*)$, $k_{**} = k(x^*, x^* | \theta^*)$, $k_* = (k(x_i, x^* | \theta^*))_{i=1}^n$, and σ^* is the optimized value of σ . Despite these simplifications, GPRs contribute significantly toward modeling various problems flexibly. However, the computational cost $\mathcal{O}(n^3)$ for the inverse matrix computation \tilde{K}^{-1} is usually unacceptable from the perspective of scalability, and the probability model $p(y | f, \Lambda)$ is unknown in some cases.

Covariance Function. The radial basis function (RBF) kernel is a basic covariance function that can be written as

$$k_{\text{rbf}}(\boldsymbol{x_s}, \boldsymbol{x_t} \mid C, \boldsymbol{l}) = C \exp\left(-\frac{1}{2}A(\boldsymbol{x_s}, \boldsymbol{x_t})\right), \quad (8)$$

$$A(\boldsymbol{x_s}, \boldsymbol{x_t}) = (\boldsymbol{x_s} - \boldsymbol{x_t})^T \operatorname{diag}(\boldsymbol{l})^{-2}(\boldsymbol{x_s} - \boldsymbol{x_t}),$$

where $\boldsymbol{l}=\{l_j\}_{j=1}^d, 0< C, l_j\in\mathbb{R}$ for all j. The covariance functions can be designed flexibly by combining multiple simpler functions. For example, Lee et al. 2018 proved that a GP with a specific covariance function is equivalent to the function of a deep neural network with infinitely wide layers. However, the covariance functions are limited to positive semi-definite types, which sometimes hinders the ability to design them freely. The Euclidean distance space (\mathbb{R}^d, d_E) between two points $(\boldsymbol{x_s}, \boldsymbol{x_t})$ in the RBF kernel $\exp(-\frac{1}{2}d_E(\boldsymbol{x_s}, \boldsymbol{x_t})^2)$ cannot be replaced by an uneven distance space (Feragen and Hauberg 2015), where $d_E: \mathbb{R}^d \times \mathbb{R}^d \to \mathbb{R}$. Some works (Guhaniyogi and Dunson 2016; Calandra et al. 2016) transformed the original feature space into a new space instead of designing the covariance function directly.

3 Likelihood-Free Gaussian Process

Here, we discuss the mechanism of the LFGP. To approximate the likelihood to a Gaussian using the asymptotic normality of the maximum likelihood estimator, we consider assigning the data points $\boldsymbol{D}=\{\boldsymbol{x_i},y_i\}_{i=1}^n$ to m clusters, i.e., $\boldsymbol{\pi}=\{\pi_i\}_{i=1}^n, \pi_i \in \{1,2,\cdots,m\}$ for all i. The maximum likelihood estimators $\hat{\boldsymbol{y}}=\{\hat{y}_h\}_{h=1}^m$ of the interest parameters $\{\hat{f}_h\}_{h=1}^m$ satisfy

$$\sum_{\substack{i\\\pi_i=h}} g'_{h,i}(\hat{y}_h) = 0,\tag{9}$$

$$q_{h,i}(\hat{f}_h) = \log p(y_i \mid \hat{f}_h, \lambda(\boldsymbol{x}_i)),$$

for all h. In this study, we assume that the random variables $\{g'_{h,i}(f(\boldsymbol{z_h}))|\pi_i=h\}$ in each cluster are independent and satisfy the Lindeberg condition (Feller 1991). If the size n_h is sufficiently large and

$$\sum_{\substack{i \\ x : -h}} \mathbb{E}_{y_i}[g'_{h,i}(f(\boldsymbol{z_h}))] = 0, \tag{10}$$

for all h, then the maximum likelihood estimators \hat{y} approximately follow the Gaussian distribution (Lehmann 1999):

$$\hat{\boldsymbol{y}} \sim \mathcal{N}(\hat{\boldsymbol{f}}, \hat{\boldsymbol{\Sigma}}),$$
 (11)

$$\hat{\sigma}_h^2 \sim \mathcal{O}(n_h^{-1}),\tag{12}$$

where $Z=\{z_h\}_{h=1}^m, z_h\in\mathbb{R}^d, \hat{f}=\{f(z_h)\}_{h=1}^m, \hat{\Sigma}=\mathrm{diag}(\hat{\sigma}_1^2, \hat{\sigma}_2^2, \cdots, \hat{\sigma}_m^2), \text{ and } 0<\hat{\sigma}_h\in\mathbb{R} \text{ for all } h.$

Proof. Using the mean-value theorem and eq. (9), we obtain

$$\hat{y}_{h} - f(\mathbf{z}_{h}) = \frac{\frac{1}{\sqrt{n_{h}}} \frac{-g'_{h}(f(\mathbf{z}_{h}))}{\sqrt{n_{h}}}}{\frac{g''_{h}(\hat{f}_{h})}{n_{h}}},$$

$$g_{h}(\hat{f}_{h}) = \sum_{\substack{i \\ \pi_{i} = h}} g_{h,i}(\hat{f}_{h}),$$
(13)

where ξ_h is between \hat{y}_h and $f(z_h)$. $\frac{g_h''(\xi_h)}{n_h} \sim \mathcal{O}(1)$. When n_h is sufficiently large, $\frac{-g_h'(f(z_h))}{\sqrt{n_h}}$ is close to a normal distribution $\mathcal{N}(0, {\sigma'}_h^2)$ for ${\sigma'}_h^2 \sim \mathcal{O}(1)$ by the central limit theorem under the assumption of independence, the Lindeberg condition and eq. (10). Therefore, $\hat{y}_h \sim \mathcal{N}(f(z_h), \hat{\sigma}_h^2)$.

Identical Parameter. We assume that $\sigma_h^2 \simeq 0$ if $n_h \geq n_0$, $\nu(\cdot) = 0$, and $k(\boldsymbol{x_i}, \boldsymbol{z_h} \mid \boldsymbol{\theta}) \simeq 0$ if $\pi_i \neq h$. Using eq. (6), we approximate $|f(x_i) - f(z_h)|$ in each cluster as

$$|f(\boldsymbol{x_i}) - f(\boldsymbol{z_h})| \simeq \left| 1 - \frac{k(\boldsymbol{x_i}, \boldsymbol{z_h} \mid \boldsymbol{\theta})}{k(\boldsymbol{z_h}, \boldsymbol{z_h} \mid \boldsymbol{\theta})} \right| |f(\boldsymbol{z_h})|.$$
 (14)

If $|f(x_i) - f(z_h)|$ is sufficiently small, then

$$g'_{h,i}(f(x_i)) \simeq g'_{h,i}(f(z_h)) + G_{h,i},$$
 (15)
 $G_{h,i} = g''_{h,i}(f(z_h))(f(x_i) - f(z_h)).$

From $\mathbb{E}_{y_i}[g'_{h,i}(f(\boldsymbol{x_i}))] = 0$, we approximate the left side of eq. (10) as

$$\sum_{\substack{i \\ \pi_i = h}} \mathbb{E}_{y_i}[g'_{h,i}(f(\boldsymbol{z_h}))] \simeq -\sum_{\substack{i \\ \pi_i = h}} \mathbb{E}_{y_i}[G_{h,i}]. \tag{16}$$

The upper bound of the absolute value of the right side of eq. (16) is

$$\left| \sum_{\substack{i \\ \pi_i = h}} \mathbb{E}_{y_i}[G_{h,i}] \right| \le G_h \sum_{\substack{i \\ \pi_i = h}} \frac{|f(\boldsymbol{x_i}) - f(\boldsymbol{z_h})|}{|f(\boldsymbol{z_h})|}, \quad (17)$$

$$G_h = \max_{i} |\mathbb{E}_{y_i}[g''_{h,i}(f(\boldsymbol{z_h}))]f(\boldsymbol{z_h})|.$$

For the assumptions of the cluster size and eq. (10), we optimize π , Z to minimize $r(\pi, Z \mid X, \theta)$ under the constraint that the size of each cluster exceeds n_0 :

$$\boldsymbol{\pi}^*, \boldsymbol{Z}^* = \underset{\boldsymbol{\pi}, \boldsymbol{Z}}{\operatorname{arg min}} r(\boldsymbol{\pi}, \boldsymbol{Z} \mid \boldsymbol{X}, \boldsymbol{\theta}), \quad (18)$$

$$r(\boldsymbol{\pi}, \boldsymbol{Z} \mid \boldsymbol{X}, \boldsymbol{\theta}) = \sum_{h} \sum_{\substack{i \\ \pi_i = h}}^{i} \left| 1 - \frac{k(\boldsymbol{x_i}, \boldsymbol{z_h} \mid \boldsymbol{\theta})}{k(\boldsymbol{z_h}, \boldsymbol{z_h} \mid \boldsymbol{\theta})} \right|.$$

Using π^* , Z^* , we state the posterior distribution of f as

$$p(\boldsymbol{f} \mid \boldsymbol{D}, \boldsymbol{\theta}, \boldsymbol{\pi}^*, \boldsymbol{Z}^*) \sim \mathcal{N}(\hat{\boldsymbol{y}} \mid \boldsymbol{f}, \hat{\boldsymbol{\Sigma}}) \mathcal{N}(\boldsymbol{f} \mid \boldsymbol{0}, \hat{\boldsymbol{K}}), \quad (19)$$
where $[\hat{\boldsymbol{K}}]_{s,t} = k(\boldsymbol{z}_s^*, \boldsymbol{z}_t^* \mid \boldsymbol{\theta}).$

Training and Prediction. The log marginal likelihood is given as

$$\hat{\mathcal{L}}(\boldsymbol{\theta} \mid \boldsymbol{D}, \boldsymbol{\pi}^*, \boldsymbol{Z}^*) = -\frac{1}{2} (\hat{\boldsymbol{y}}^T \hat{\boldsymbol{K}}^{-1} \hat{\boldsymbol{y}} + \log |\hat{\boldsymbol{K}}| + c).$$
(20)

We optimize θ to maximize the log marginal likelihood:

$$\theta^* = \underset{\theta}{\operatorname{arg max}} \hat{\mathcal{L}}(\theta \mid D, \pi^*, Z^*).$$
 (21)

The mean and variance of the posterior distribution of $f^* =$ $f(x^*)$ for a new input x^* are

$$\mathbb{E}[f^* \mid D, \theta^*, \pi^*, Z^*] = \hat{k}_*^T \hat{K}_*^{-1} \hat{y}, \tag{22}$$

$$Var[f^* \mid D, \theta^*, \pi^*, Z^*] = k_{**} - \hat{k}_*^T \hat{K}_*^{-1} \hat{k}_*,$$
 (23)

where $[\hat{K}_*]_{s,t} = k(z_s^*, z_t^* \mid \theta^*), k_{**} = k(x^*, x^* \mid \theta^*),$ and $\hat{k}_* = (k(z_h^*, x^* \mid \theta^*))_{h=1}^m$. It is usually infeasible to optimize θ directly because π^*, Z^* depend on θ . Therefore, we decompose the optimization process into two iterative processes as in algorithm 1. The process of the log marginal likelihood maximization is usually reasonable because the computational cost of the inverse matrix is $\mathcal{O}(\frac{n^3}{n_0^3})$. However, distance-based clustering is generally difficult for scalability reasons.

Algorithm 1 Hyperparameter optimization

1: Input:
$$D = \{X, y\}, n_0, \epsilon, \theta$$
 Output: θ_{old}, π, Z

3:
$$\theta_{\text{old}} \leftarrow \theta$$

2. Repeat

3:
$$\theta_{\text{old}} \leftarrow \theta$$

4: $\pi, Z \leftarrow \underset{\substack{\pi, Z \\ n_1, n_2, \cdots, n_m \geq n_0}}{\arg \min} r(\pi, Z \mid D, \theta)$

5: $\theta \leftarrow \underset{\theta}{\arg \max} \hat{\mathcal{L}}(\theta \mid D, \pi, Z)$

$$n_1, n_2, \cdots, n_m \ge n_0$$

5:
$$\boldsymbol{\theta} \leftarrow \arg \max \hat{\mathcal{L}}(\boldsymbol{\theta} \mid \boldsymbol{D}, \boldsymbol{\pi}, \boldsymbol{Z})$$

6: until
$$\hat{\mathcal{L}}(\boldsymbol{\theta} \mid \boldsymbol{D}, \boldsymbol{\pi}, \boldsymbol{Z}) - \hat{\mathcal{L}}(\boldsymbol{\theta}_{old} \mid \boldsymbol{D}, \boldsymbol{\pi}, \boldsymbol{Z}) \leq \epsilon$$

Clustering

To reduce the difficulties associated with scalable clustering, we set the RBF kernel to the covariance function. The form of eq. (18) is expressed as follows:

$$oldsymbol{\pi_{\mathbf{rbf}}^*}, oldsymbol{Z_{\mathbf{rbf}}^*}^* \simeq \mathop{\arg\min}_{\substack{oldsymbol{\pi}, oldsymbol{Z} \\ n_1, n_2, \cdots, n_m \geq n_0}} \sum_{h} \sum_{\substack{i \\ \pi_i = h}} A(oldsymbol{x_i}, oldsymbol{z_h}). \quad (24)$$

This is equivalent to the linear k-means (Hartigan and Wong 1979) function, which is computationally light because we can obtain the centroids analytically. The computational cost is given by $\mathcal{O}(nm)$ (Murphy 2012). However, the two discussion points are the size constraint of the clusters generated by linear k-means and representation of the uneven distance.

Constraint. We can obtain the solution of the linear k-means function heuristically and efficiently using the expectationmaximization algorithm. However, assigning data points to clusters under the cluster size constraints is usually difficult. Here, we provide algorithm 2 by applying the idea of x-means (Pelleg and Moore 2000), which recursively splits a cluster into two clusters via linear k-means until the clusters no longer meet the division conditions. This algorithm enables us to retain the cluster size constraint while maintaining efficiency in the linear k-means process. The computational cost of algorithm 2 is $\mathcal{O}(\frac{n^2}{n_0})$. Therefore, the total cost of algorithm 1 is $\mathcal{O}(\frac{n^2}{n_0}) + \mathcal{O}(\frac{n^3}{n_0^3})$.

Manifold. As shown above, the RBF kernel significantly reduces the computational cost of algorithm 2. However, we cannot guarantee that we can appropriately represent the feature space by the RBF kernel. Here, the RBF kernel is not capable of representing the uneven distance of the feature space, as the covariance matrix must be semi-positive definite. This is a critical drawback when the data points are distributed on manifolds (\mathcal{M}, d_M) embedded in Euclidean space (\mathbb{R}^d, d_E) . To overcome this drawback, we convert the original feature space into a new Euclidean space that approximately preserves the uneven distances as an option of the LFGP. For this conversion, we use manifold learning methods (e.g., locally linear embedding (LLE) (Saul and Roweis 2001), Isomap (Schoeneman et al. 2018), and UMAP (McInnes and Melville 2018)) that represent the manifold distances among data points based on the k-neighbor graph.

Algorithm 2 Recursive clustering

```
1: Input: X Output: \pi, Z \leftarrow \operatorname{RC}(X)

2: procedure \operatorname{RC}(X)

3: if 2n_0 > |X| then

4: return assignment number and centroids.

5: else

6: Split X into two clusters X_1, X_2.

7: if \min\{|X_1|, |X_2|\} < n_0 then

8: split X into X_1, X_2 evenly and randomly.

9: Run \operatorname{RC}(X_1), \operatorname{RC}(X_2) recursively.
```

5 Experimental Results

Here, we present two experimental results that verify the performance of the LFGP. The computing environment used is Microsoft Windows 10 Pro,3.6 GHz Intel Core i9 processor, and 64 GB memory. The code to replicate each experiment in this study is available ¹.

5.1 Basic Performance

In this subsection, we present the verification of the behavior of the LFGP from two perspectives using pseudo datasets. First, we determine the representations of the posterior distributions of some interest parameters. Our interest parameters here depend on the individual problems. The LFGP allows us to represent the posterior distribution of various types of parameters flexibly. Second, we convert the original feature space into a new Euclidean space using manifold learning methods. The feature space sometimes

has the structure of a manifold embedded in Euclidean space. However, in the framework of the LFGP, kernels are difficult to use practically, except for the RBF kernel, owing to the computational cost of clustering for scalability. We show empirically that a preprocessing conversion before training reduces this drawback.

Setup. We prepared two pseudo datasets (Cube and Roll), which are plotted in n data points as indicated in table 1. The parameters mapped by f are the mean, median, variance, and skew, and they do not give the information of the beta distribution directly. Under these experimental conditions, we first train the LFGP on each dataset. Additionally, in the case of Roll, we convert the feature space using each of LLE, Isomap, and UMAP. Next, we show the mean of the posterior distribution of each parameter on $n^* = 30$ test data points, replacing n, x_i in table 1 with n^*, x_i^* .

Table 1: Pseudo Dataset

| Type | $x_{i,1}$ | $x_{i,2}$ | $x_{i,3}$ | y_i |
|--------------|---|--|--------------------|---|
| Cube Roll | $\frac{-n+2i}{n} \cos \frac{2i}{n} \pi$ | $\frac{\mathrm{U}(0,1)}{\frac{i}{n}\sin\frac{2i}{n}\pi}$ | $U(0,1) \\ U(0,1)$ | $\frac{\operatorname{Be}(\frac{n+i}{n}, \frac{4n-3i}{n})}{\operatorname{Be}(\frac{n+i}{n}, \frac{4n-3i}{n})}$ |

Baseline. We replace $\pi_{\mathbf{rbf}}^*, Z_{\mathbf{rbf}}^*$ of eq. (24) with

$$\pi_{\mathbf{base}}^*, \mathbf{Z}_{\mathbf{base}}^* = \underset{\substack{\pi, \mathbf{Z} \\ n_1, n_2, \dots, n_m \ge n_0}}{\operatorname{arg \, min}} \sum_{\substack{h \\ \pi_i = h}} B(\mathbf{x}_i, \mathbf{z}_h), (25)$$

$$B(\mathbf{x}_i, \mathbf{z}_h) = (\mathbf{x}_i - \mathbf{z}_h)^T (\mathbf{x}_i - \mathbf{x}_h).$$

Through a comparison to this, we verify that the clustering based on eq. (18) contributes to Gaussian approximation.

Performance. From fig. 1, the LFGP in the case of Cube is close to the true value of each parameter. On the other hand, the baseline in the case of Cube is away from the true value. Figure 2 is the result without manifold learning methods in the case of Roll. As the training data size n increases, the performance improves even if we do not convert the feature space by manifold learning methods. However, the performance without manifold learning methods is poor when the feature space has a manifold structure and the training data size n is small. Figure 3 is the result with manifold learning methods in the case of Roll. The conversion of the feature space by manifold learning methods tends to improve the performance even if the training data size n is small. Isomap improves the performance even if the training data size n is small. However, the performance with UMAP is equal to or worse than that without manifold learning methods. The LFGP with LLE is close to the true value of each parameter. On the other hand, the baseline with LLE is slightly away from it. These results suggest that the LFGP improves the performance to represent the posterior distribution of parameters and it is necessary to convert the feature space appropriately depending on the specific problem. In addition, table 2 shows that we can train the LFGP on scalable problems in a realistic timeframe.

¹https://github.com/MLPaperCode/LFGP

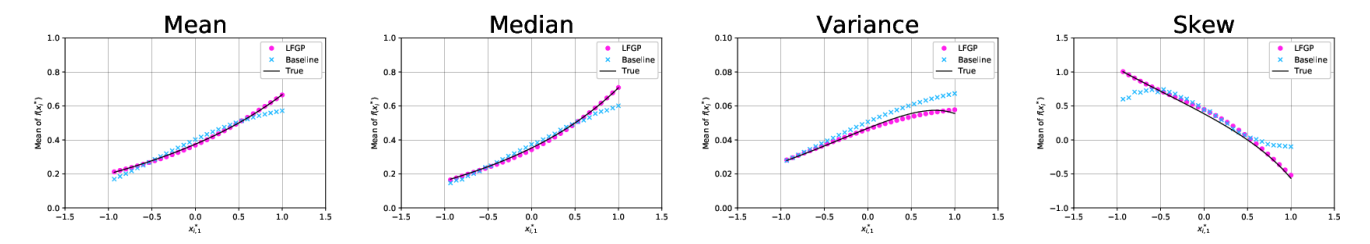


Figure 1: Mean of $f(\boldsymbol{x_i^*})$ against $x_{i,1}^*$ when the pseudo dataset is **Cube** and the feature space is **not converted** by manifold learning methods. $n=10,000, d=3, n_0=1000, n^*=30$, and $\epsilon=1$.

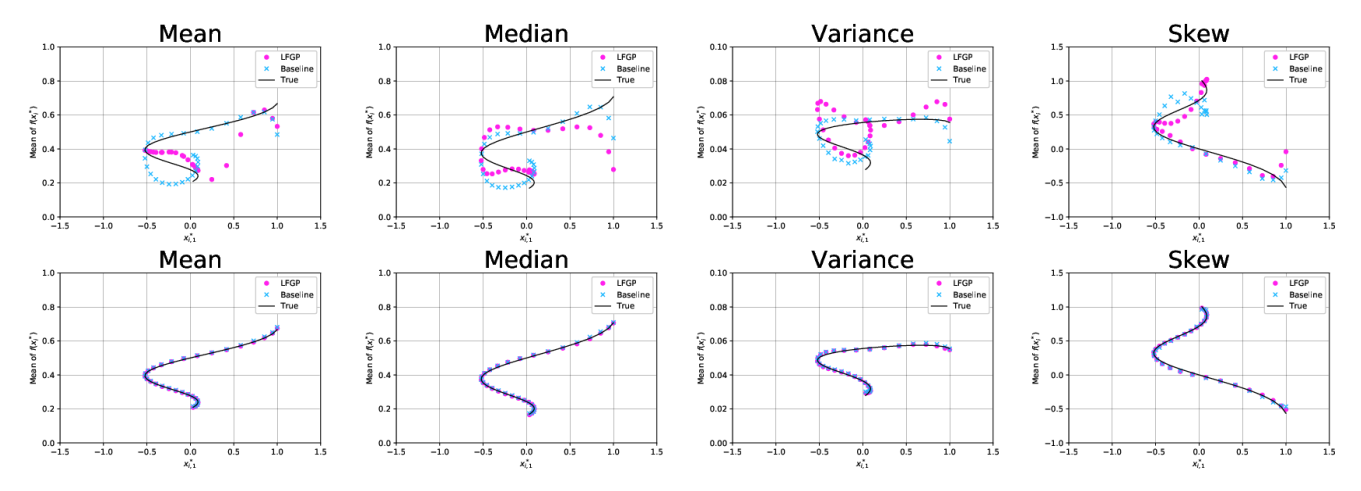


Figure 2: Mean of $f(x_i^*)$ against $x_{i,1}^*$ when the pseudo dataset is **Roll** and the feature space is **not converted** by manifold learning methods. Upper: n=10,000. Lower: n=100,000. $d=3,n_0=1000,n^*=30$, and $\epsilon=1$.

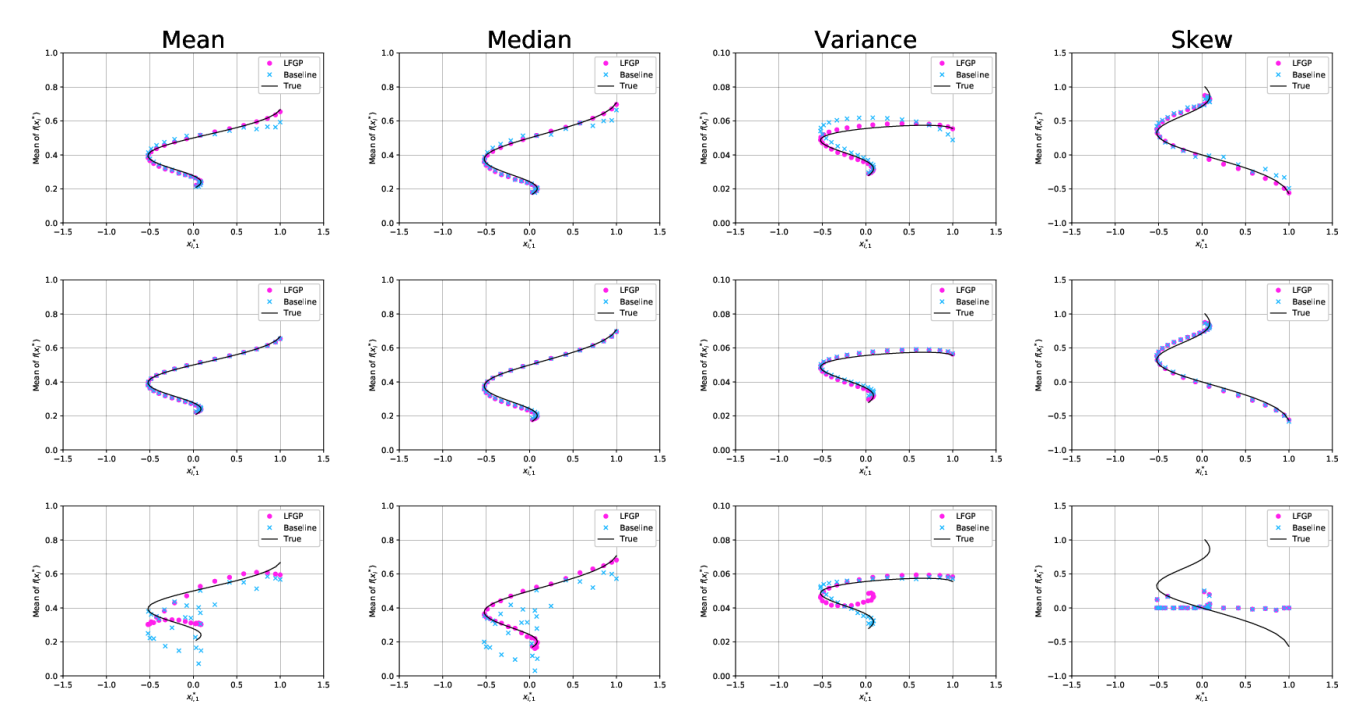


Figure 3: Mean of $f(x_i^*)$ against $x_{i,1}^*$ when the pseudo dataset is **Roll** and the feature space is **converted** by manifold learning methods. Upper: LLE. Middle: Isomap. Lower: UMAP. $n=10,000, d=3, n_0=1000, n^*=30, \epsilon=1$, and the k-neighbors of each case is 50.

Table 2: Calculation time and repetition count of algorithm 1. All numerical values in this table are averaged over 10 trials for the cases of Cube, mean, and non-conversion. d=3 and $\epsilon=1$.

| | $n_0 = 100$ | | $n_0 = 1,000$ | | $n_0 = 10,000$ | |
|---|--|---|--|---|---|---|
| n | training time [s] | repetition count | training time [s] | repetition count | training time [s] | repetition count |
| 100,000 200,000 400,000 800,000 1,600,000 | 41 ± 8 91 ± 24 257 ± 65 720 ± 60 $3,048 \pm 666$ | 2.7 ± 0.7 2.0 ± 1.1 2.0 ± 0.8 1.7 ± 0.5 1.9 ± 0.6 | 6 ± 1 15 ± 3 36 ± 6 87 ± 15 175 ± 21 | 1.3 ± 0.5 1.3 ± 0.5 1.4 ± 0.5 1.6 ± 0.5 1.1 ± 0.3 | 3 ± 1 9 ± 1 24 ± 2 42 ± 1 100 ± 1 | 1.4 ± 0.5 1.8 ± 0.4 1.9 ± 0.3 1.0 ± 0.0 1.0 ± 0.0 |

5.2 Binary Option

It is generally infeasible to model asset price fluctuations because their probability models are unknown. Herein, we suggest that the LFGP enables representing the percentile points of currency exchange rate fluctuations. To verify the performance of the LFGP, we consider the BO index, which is a simple derivative instrument. The BO index is generally above or below the currency exchange rate fluctuations at any given time. The cash flow of the BO is binary in nature, despite being based on the currency exchange rates. Therefore, we can model the cash flow from the BO directly without representing the percentile points of the currency exchange rate fluctuations. Using this feature of the BO, we compare the performance of each direct and indirect representation obtained via LFGP of the cash flow from the BO. The historical currency exchange rate used here is from OANDA API².

Rule. In this experiment, we consider the following rules for the BO:

- 1. Predict whether a currency exchange rate will increase or decrease 30 s in advance.
- 2. Payout is 1.95 for 1 entry cost if the prediction is correct.
- 3. A draw is treated as incorrect (significant digits: 0.1 pips).
- 4. Possible entry timing is Monday to Friday, 8:00-29:00, except for New Year and holidays.

This rule is based on HighLow³

Strategy. The whole procedure is simple:

- 1. Represent each $\frac{95}{195} \times 100$ and $\frac{100}{195} \times 100$ percentile point every 1 min with the LFGP based on every 30 s of rate fluctuation for the previous 30d s.
- 2. Add stress to the mean of the percentile points based on the posterior distribution,

$$\int_{-\infty}^{f_H^*} \mathcal{N}(f_H \mid m_H, k_H) df_H = \alpha, \tag{26}$$

$$\int_{-\infty}^{f_H^*} \mathcal{N}(f_H \mid m_H, k_H) df_H = \alpha, \qquad (26)$$

$$\int_{-\infty}^{f_L^*} \mathcal{N}(f_L \mid m_L, k_L) df_L = 1 - \alpha, \qquad (27)$$

where f_H, f_L are the $\frac{95}{195} \times 100, \frac{100}{195} \times 100$ percentile points of the currency exchange rate fluctuations in 30s; f_H^*, f_L^* are $\alpha, 1 - \alpha$ percentile points of f_H, f_L ; $(m_H, k_H), (m_L, k_L)$ are the mean and variance of the posterior distribution of f_H , f_L ; and α represents the degree of stress, $0 < \alpha \le 0.5, \alpha \in \mathbb{R}$.

3. Bet High if f_H^* is more than 0.05 pips and bet Low if f_L^* is less than -0.05 pips.

We bet on GBP/JPY. The frequency of draws in GBP/JPY is low compared to other currencies because the volatility of it is high. We train the LFGP as a nonparametric model under the hypothesis that there are some patterns of rate movements in short intervals. We do not convert the feature space before the training because of the lack of knowledge of the feature space.

Baseline. For the proposal method, we represent the percentile points of the currency exchange rate fluctuations. Instead of the proposal method, we model the cash flow from the BO directly as a baseline. Here, a draw is treated as incorrect. Therefore, the currency exchange rate fluctuations are classified into three patterns: up, down, and flat. We represent the individual probabilities of High and Low obtained by LFGP. The strategy in this case is almost the same as that of the proposal method, but we replace each $\frac{95}{195} \times 100$ and $\frac{100}{195} \times 100$ percentile point with each probability of High and Low. We bet High if the probability of High is more than 0.5 and bet Low if the probability of Low is more than 0.5.

Evaluation. The training period is 2017/9/1–2018/8/31, and the evaluation period is 2018/9/1–2019/8/31. We search the parameters that maximize the cumulative profit for the evaluation period. The candidates of the parameters are d = 10, 20, 30 and $n_0 = 100, 200, 300$. As a result of this evaluation, the proposal method with $d = 10, n_0 = 100$ maximized the cumulative profit for the evaluation period (313,794 rounds for the evaluation and 315,043 rounds for the training). The baseline with $d = 30, n_0 = 200$ maximized it (311,284 rounds for the evaluation and 312,513 rounds for the training). From fig. 4, the level of the cumulative profit in the cases of the proposal method and the baseline is different. However, the behavior in both cases is similar: the smaller (i.e. higher stress) α is, the greater the ratio of the cumulative profit to entry count is.

²https://developer.oanda.com/rest-live-v20/introduction/

³https://trade.highlow.com/

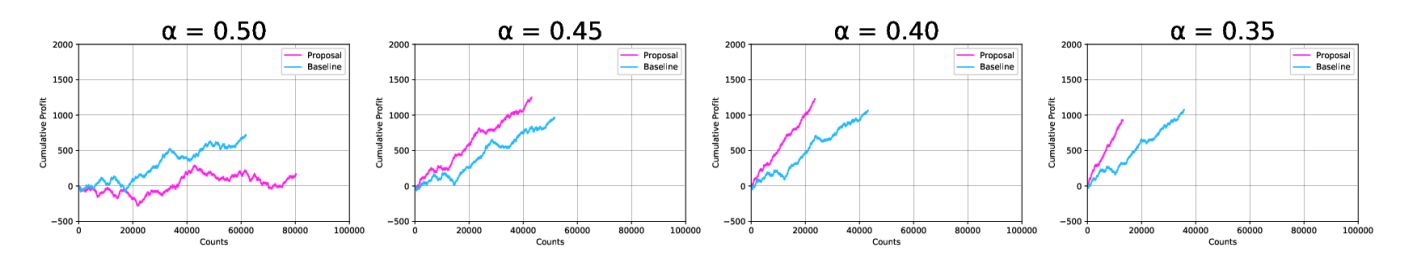


Figure 4: Evaluation results for the period 2018/9/1–2019/8/31. Cumulative profit against entry counts for each α . Training period is 2017/9/1–2018/8/31. Proposal: $d=10, n_0=100, 313,794$ rounds for evaluation, and 315,043 rounds for training. Baseline: $d=30, n_0=200, 311,284$ rounds for evaluation, and 312,513 rounds for training. $\epsilon=1$.

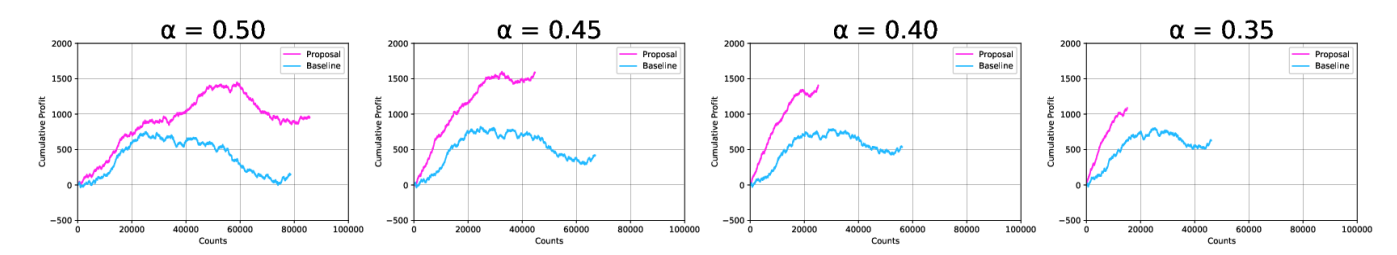


Figure 5: Backtesting results for the period 2019/9/1–2020/8/31. Cumulative profit against entry counts for each α . Training period is 2018/9/1–2019/8/31. Proposal: $d=10, n_0=100, 315,409$ rounds for backtesting, and 313,794 rounds for training. Baseline: $d=30, n_0=200, 312,889$ rounds for backtesting, and 311,284 rounds for training. $\epsilon=1$.

Backtesting. The training period is 2018/9/1–2019/8/31, and the backtesting period is 2019/9/1-2020/8/31. From the evaluation result, we used $d = 10, n_0 = 100$ for the proposal method (315,409 rounds for backtesting and 313,794 rounds for training), and $d = 30, n_0 = 200$ for the baseline (312,889 rounds for backtesting and 311,284 rounds for training). Figure 5 shows that the behavior of the ratio of the cumulative profit to the entry count for each α is similar to that of fig. 4 in the cases of the proposal method and the baseline. We cannot conclude that the proposal method is superior to the baseline as a BO trading model from this result alone. However, this result suggests that the LFGP can represent the posterior distribution of percentile points without knowledge of the probability distribution of the currency exchange rate fluctuation. The performance in the second half of the entry is poor except for when α is small. We assume that this is caused by the COVID-19 Pandemic, which has changed global economic trends significantly.

6 Conclusion

In this study, we proposed the LFGP, which is a framework for likelihood-free modeling. The main concept of the LFGP is representation in the form of a typical GPR by the approximation of the likelihood in each cluster to a Gaussian using the asymptotic normality of the maximum likelihood estimator. The clustering to obtain the maximum likelihood estimators of an interest parameter is based on the distance obtained by the covariance function. We suggested theoretically and experimentally that the distance obtained by the

covariance function increases the accuracy of the Gaussian approximation. Compared to existing methods, the LFGP contributes to fewer assumptions for the probability models, which enables us to represent the posterior distribution of an interest parameter even if only little knowledge on its probability model is available. However, the computational cost to set up such clusters is usually infeasible. To reduce this computational disadvantage, we used RBF kernel as the covariance function. In this case, clustering according to distance based on the covariance function is equivalent to k-means, which is computationally reasonable. Furthermore, we solved the cluster size constraints using x-means and represented the uneven space using manifold learning methods.

We expect that the LFGP will contribute to likelihoodfree modeling in several fields. One typical application is the modeling of cash flows for investing in financial instruments. The cash flows of financial instruments are usually quite complex, which makes it difficult to establish trading models for them. Using BO, we suggested experimentally that LFGP can represent the posterior distribution of the percentile points of currency exchange rate fluctuation. It is not necessary to use the LFGP for BO trading because we know that the probability model of BO cash flow is a binary distribution. However, we consider that the LFGP will help improve the performance of trading for other assets. Presently, we are continuing our experiments to gain actual profits from the foreign exchange (FX), not only via backtesting. We expect to report the results of the extended work in the near future.

Ethics Statement

This study could have a positive impact in terms of stimulating the investment market. Novice investors should learn numerous techniques, which is sometimes a barrier to joining in investment markets. Algorithmic trading might reduce the barrier with a lower fee than professional funds. Further, a concentration risk may occur if investors use similar algorithmic trading models. We should be cautious as algorithmic trading could break the investment market.

Acknowledgement

I wish to thank Dr. Naoki Hamada, Dr. Junpei Komiyama, Dr. Takashi Ohga, Atsushi Suyama, Kevin Noel, Tomoaki Nakanishi, Kohei Fukuda, Masahiro Asami, Daisuke Kadowaki, Yuji Hiramatsu, Hirokazu Iwasawa, and Korki Tomizawa for invaluable advice provided during the writing of this paper. I would also like to thank Editage for their high-quality English language editing. I am grateful to my family for supporting my research activities.

References

- Bui, T. D.; and Turner, R. E. 2014. Tree-structured Gaussian process approximations. In *Proceedings of the 27th International Conference on Neural Information Processing Systems*, 2213–2221. Cambridge, MA, USA: MIT Press.
- Calandra, R.; Peters, J.; Rasmussen, C. E.; and Deisenroth, M. P. 2016. Manifold Gaussian processes for regression. In *Proceedings of International Joint Conference on Neural Networks*, 3338–3345. Vancouver, BC, Canada: IEEE.
- Candela, J. Q.; and Rasmussen, C. E. 2005. A unifying view of sparse approximate Gaussian process regression. *Journal of Machine Learning Research* 6: 1939–1959.
- Csat, L.; and Opper, M. 2000. Sparse representation for Gaussian process models. In *Proceedings of the 13th International Conference on Neural Information Processing Systems*, 423–429. Cambridge, MA, USA: MIT Press.
- Feller, F. 1991. An Introduction to Probability Theory and Its Applications, volume 2. 2 edition.
- Feragen, A.; Lauze, F.; and Hauberg, S. 2015. Geodesic exponential kernels: When curvature and linearity conflict. In *Proceedings of Computer Vision and Pattern Recognition*, 3032–3042. Boston, MA, USA: IEEE.
- Guhaniyogi, R.; and Dunson, D. B. 2016. Compressed Gaussian process for manifold regression. *Journal of Machine Learning Research* 17(1): 2472–2497.
- Gutmann, M. U.; and Corander, J. 2016. Bayesian optimization for likelihood-free inference of simulator-based statistical models. *Journal of Machine Learning Research* 17(125): 1–47.
- Hartigan, J. A.; and Wong, M. A. 1979. A k-means clustering algorithm. *Applied statistics* 28(1): 100–108.
- Hensman, J.; Matthews, A. G.; Filippone, M.; and Ghahramani, Z. 2015. MCMC for variationally sparse Gaussian processes. In *Proceedings of the 28th International Conference on Neural Information Processing Systems*, 1648–1656. Cambridge, MA, USA: MIT Press.

- Lee, J.; Bahri, Y.; Novak, R.; Schoenholz, S. S.; Pennington, J.; and Sohl-Dickstein, J. 2018. Deep neural networks as Gaussian processes. In *Proceedings of International Conference on Learning Representations*. Vancouver, BC, Canada.
- Lehmann, E. L. 1999. *Elements of Large-Sample Theory*. Springer.
- McInnes, L.; Healy, J.; and Melville, J. 2018. UMAP: Uniform manifold approximation and projection for dimension reduction. *Journal of Open Source Software* 3(29).
- Murphy, K. P. 2012. *Machine Learning: A Probabilistic Perspective*. MIT Press.
- Pelleg, D.; and Moore, A. W. 2000. X-means: Extending K-means with efficient estimation of the number of clusters. In *Proceedings of International Conference on Machine Learning*, 727–734. Morgan Kaufmann Publishers.
- Rasmussen, C. E.; and Williams, C. K. I. 2006. *Gaussian Processes for Machine Learning*. MIT Press.
- Saul, L. K.; and Roweis, S. T. 2001. An introduction to locally linear embedding. *Journal of Machine Learning Research* 7.
- Schoeneman, F.; Chandola, V.; Napp, N.; Wodo, O.; and Zola, J. 2018. Entropy-Isomap: Manifold learning for high-dimensional dynamic processes. In *Proceedings of IEEE International Conference on Big Data*. IEEE.
- Shen, Y.; Ng, A.; and Seeger, M. 2005. Fast Gaussian process regression using KD-trees. In *Proceedings of the 18th International Conference on Neural Information Processing Systems*, 1225–1232. Cambridge, MA, USA: MIT Press.
- Sidehabi, S. W.; Amirullah, I.; and Tandungan, S. 2016. Statistical and machine learning approach in forex prediction based on empirical data. In *Proceedings of International Conference on Computational Intelligence and Cybernetics*. IEEE.
- Thu, T. N. T.; and Xuan, V. D. 2018. FoRex trading using supervised machine learning. *International Journal of Engineering and Technology* 7(4.15): 400–404.
- Titsias, M. K. 2009. Variational learning of inducing variables in sparse Gaussian processes. *Proceedings of Machine Learning Research* 5: 567–574.
- Wood, S. N. 2010. Statistical inference for noisy nonlinear ecological dynamic systems. *NATURE* 466(7310): 1102–1104.